Primljen / Received: 15.1.2024.
Ispravljen / Corrected: 5.8.2024.
Prihvaćen / Accepted: 16.8.2024.
Dostupno online / Available online: 10.11.2024.

# Nonlinear response of RC column models under real earthquakes and axial loads

Authors:

Asst.Prof. **Zijadin Guri**, PhD. CE
University of Pristina
Faculty of Civil Engineering and Architecture
zijadin.guri@uni-pr.edu
**Corresponding author**

Assoc.Prof. **Jelena Ristić**, PhD. CE
International Balkan University (IBU), Skopje
Faculty of Engineering
Department of Civil Engineering
jelena.ristic@ibu.edu.mk

Prof. **Danilo Ristić**, PhD. CE
University of St. Cyril and Methodius, Skopje
Institute of Earthquake Engineering and Engineering Seismology (IZIIS)
danilo.ristic@gmail.com

Research Paper

Zijadin Guri, Jelena Ristic, Danilo Ristic

## Nonlinear response of RC column models under real earthquakes and axial loads

This paper reports on original findings from advanced HYLSER-1 seismic tests conducted on steel-reinforced concrete column models subjected to simulated low and high axial loads. The study includes a comparative analysis of steel-reinforced concrete (SRC) column models and composite-reinforced concrete (CRC) column models, using refined nonlinear analytical micro-models. The results demonstrate that earthquake intensity, axial load level, and concrete confinement are the primary factors influencing the complex hysteretic responses and failure of column models reinforced with either conventional steel bars or novel glass fibre-reinforced polymer (GFRP) bars. These findings are crucial for enhancing the seismic design of alternatively reinforced columns subjected to severe earthquakes.

**Key words:**
**concrete, columns, steel bars, GFRP bars, testing, earthquakes, nonlinear response**

Prethodno priopćenje

Zijadin Guri, Jelena Ristić, Danilo Ristić

## Nelinearni odziv modela AB stupova uslijed stvarnih potresa i osnih opterećenja

U ovom su radu predstavljeni izvorni rezultati iz naprednih seizmičkih ispitivanja sustavom HYLSER-1, provedenih na modelima armiranobetonskih stupova podvrgnutim simuliranim manjim i većim osnim opterećenjima. Ovo istraživanje obuhvaća komparativnu analizu modela armiranobetonskih (AB) stupova i modela kompozitnih armiranobetonskih stupova (eng. *composite-reinforced concrete* - CRC) primjenom detaljnih nelinearnih analitičkih mikromodela. Rezultati pokazuju da su intenzitet potresa, razina osnog opterećenja i ovijanje betona primarni čimbenici koji utječu na složeni histerezni odziv i lom modela stupova armiranih uobičajenim čeličnim šipkama ili šipkama od polimera ojačanog staklenim vlaknima (GFRP). Ova su otkrića presudna za poboljšanje projektiranja potresne otpornosti alternativno armiranih stupova izloženih jakim potresima.

**Ključne riječi:**
**beton, stupovi, čelične šipke, GFRP šipke, ispitivanje, potresi, nelinearni odziv**

## 1. Introduction

In seismic regions, the safety of structures largely depends on the seismic performance of their columns, making it crucial to understand their seismic response characteristics. Traditionally, steel bars have been used as reinforcement in reinforced concrete (RC) columns. However, recent research has focused on using fibre-reinforced polymer (FRP) bars to prevent corrosion in aggressive environments. To design steel and FRP-reinforced columns that can withstand large seismic loads and exhibit significant nonlinear responses, it is essential to fully understand how various design parameters affect their hysteretic response characteristics.

Due to the specific characteristics of columnar structures (e.g., bridges, complex buildings) and the unpredictable nature of ground-motion excitation, columns are primarily subjected to a combination of seismically induced bending and axial loading [1]. Studies on the bidirectional response of RC columns under constant axial load have demonstrated that bidirectional loading reduces drift capacity and accelerates the degradation of strength and stiffness [2-6]. Tests have shown that the axial load ratio of a column's cross-section, (i.e. $S = N/\sigma_c A_c$) significantly affects its relative displacement capacity [4, 7, 8]. According to the drift model [9, 10], increasing the axial load ratio from 0.1 to 0.3 reduces displacement capacity by a factor of 2.3. Therefore, inadequate consideration of axial load effects in design can lead to damage or even total collapse of columns during strong earthquakes. In such cases, complex and costly strengthening and repair techniques are required to enhance the strength and ductility of columns. These techniques include RC jacketing, steel jacketing, externally bonded FRP, near-surface mounted FRP, shape memory alloy jacketing, and hybrid jacketing, as recently presented [11, 12]. Due to their advanced mechanical properties and proven durability, FRP bars have recently been introduced as an alternative form of internal reinforcement. FRP-reinforced elements are commonly used in RC structures and bridges exposed to aggressive environmental conditions [13]. Advantages of FRP bars over steel bars include a higher strength-to-weight ratio, electromagnetic neutrality, high cutting ability for temporary applications, and their lightweight, flexible nature. Most FRP bars are made from carbon (CFRP), glass (GFRP), or aramid (AFRP) fibres [14, 15]. Notably, extensive research has focused on the mechanical properties of GFRP bars, particularly their compressive strength, which is typically 55 % to 65 % of their tensile strength [16, 17]. The compressive and tensile strengths are primarily influenced by fibre volume and type, resin material, and the manufacturing process, while the modulus of elasticity remains approximately the same in both compression and tension [18]. Recent studies have separately examined the behaviour of columns reinforced with GFRP bars and those reinforced with steel bars [13,19, 20]. For a given amount of longitudinal reinforcement, members reinforced with GFRP bars experience more significant cracking and displacement under flexure compared to those reinforced with steel bars (Nanni, 1993). GFRP bars contribute less to the axial capacity of columns than steel bars, and using FRP reinforcement instead of steel does not enhance the compressive capacity of columns but does delay the buckling of longitudinal bars [13, 21, 22]. The bending-moment and axial-load capacities of columns reinforced with steel bars are higher than those of columns reinforced with GFRP bars, although both types exhibit similar ductility [19, 20, 23]. Since the compression modulus of GFRP bars is lower than their tension modulus, many authors and design codes [16] advise against using them as compressive reinforcement in columns and beams. The Canadian design code [17] permits GFRP reinforcement for compressive applications but recommends that the strength of the compressed bars should not be included in the capacity calculations of structural elements. While various studies have examined concrete columns reinforced with either steel or GFRP bars, relatively few comparative studies using the same models exist.

Given the severe and unacceptable damage observed in columns under earthquake-induced complex loading, studying the seismic safety of both traditional and innovative GFRP-reinforced columns is a crucial and continually relevant research topic. This study aims to leverage our unique previous study results obtained from extensive HYLSER-1 experimental tests and advanced micro-modeling concepts to generate new and significant scientific insights.

**a) Testing advances with HYLSER-1 system:** The tests conducted using the Hybrid Loading System of Earthquake Response-1 (HYLSER-1) represent a specific experimental study carried out in Japan, involving original research by the third author. The HYLSER-1 testing system enabled realistic simulation of the inelastic seismic response of RC column models under the simulated effects of severe earthquakes, while also incorporating the interactive effects of specified axial loads. Through a well-designed testing programme, the effects of various influencing parameters were experimentally investigated, including:

*Old experiments for new scientific benefits:* Given the advancements in modern software and micro-modeling, coupled with the valuable results from previous HYLSER-1 experiments, the conditions are now ideal to conduct this specific research after many years.

*Low axial load:* The earthquake response of models under low, constant axial load was verified by simulating various levels of concrete strength, confinement, and earthquake intensity.

*High axial load:* Similarly, the earthquake response of models under high, constant axial load was verified by considering the same varying parameters.

*Low and high earthquake intensity:* By simulating low and high earthquake intensities, the hysteretic responses and damage states of the tested models were assessed.

*Concrete strength and confinement:* The effects of concrete strength and confinement on the tested columns were identified and presented in the respective tables.

**b) Modelling advances:** Significant advances in modelling have been demonstrated through the accurate prediction of hysteretic responses for the same tested models.
*Common and composite columns under low and high axial load:* Using refined and experimentally validated analytical micro-models, the hysteretic responses of reinforced columns with both conventional and novel composite reinforcements were predicted and compared under simulated low and high constant axial loads.
*Axial load effect to common and composite columns:* The original analytical results clearly demonstrated the actual effects of axial load on columns reinforced with both conventional and composite reinforcements.

**c) Importance and research novelty:** The recent intolerable seismic damage and total collapse of columns in earthquakes highlight the significance and novelty of this research. This comprehensive study aims to provide a valuable, experimentally validated contribution that addresses and fills the existing research gap.
*Filling the research gap:* Given the increased practical application of both conventional and novel columns, there is a clear need for a systematic comparative evaluation of the differences in hysteretic responses between commonly reinforced columns and those reinforced with composite materials. This study was initiated and completed to provide original results and address the existing research gap.
*Flow of multitask research:* The study comprised several specific research phases, including: 1) processing results from HYLSER-1 seismic tests with simulated low and high axial loads; 2) analytically predicting the hysteretic responses of commonly reinforced columns and those reinforced with novel GFRP bars under low and high axial loads; 3) experimentally validating the formulated nonlinear micro-model; and 4) deriving original conclusions and recommendations.
*Summary of novel results:* For the future design of columns reinforced with both conventional steel and novel GFRP bars in seismic areas, the effects of various involved variables were evaluated and presented.
*Step toward advanced applications:* Based on the original comparative results, the practical design of columns reinforced with either conventional steel or novel GFRP bars in seismic areas can be significantly improved. In this context, it is also recommended to update the existing seismic design provisions.

The paper presents results from original earthquake response tests on scaled prototype column models subjected to simulated axial loads. These results are compared with those from refined analytical studies of the nonlinear responses of the same models, reinforced with either steel or GFRP bars, based on experimentally validated nonlinear models [14, 15].

## 2. Study objectives and methodology

Concrete columns reinforced with steel bars have been widely used in practice. However, inadequate design has led to significant damage or even collapse of RC columns in past earthquakes. To address corrosion issues in aggressive environments, novel concrete columns reinforced with FRP bars have recently emerged as a reliable alternative in construction practice [16]. This research aims to comparatively evaluate the performance up to failure of both types of columns subjected to bending and axial loads. The study integrates experimental and analytical approaches to address existing design and research gaps. Given the complexity of the research objectives, the study involved comprehensive experimental and analytical investigations using the same column models and loading conditions.

## 3. Implemented hybrid loading system for earthquake response

The hybrid or pseudo-dynamic HYLSER-1 seismic testing method was originally developed based on a specific experimental concept established by the research team, including the third author.

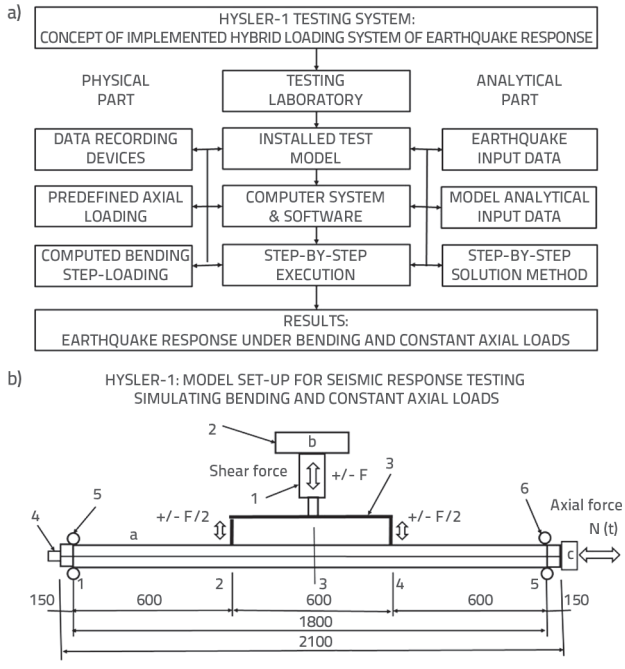


**Figure 1. HYLSER-1 testing system (Kyoto-Lab): a) concept of hybrid loading system for earthquake response; b) test setup for testing column models under simulated earthquake and axial loads**

The method remains popular due to its low cost and its ability to combine the benefits of shaking-table testing with additional

specific advantages. The earliest pseudo-dynamic testing systems were introduced in Japan [24–27]. In a hybrid seismic-response test, the system integrates a lab-analytical approach, with column models serving as the core laboratory component. For the defined combined lab-analytical system and selected earthquake record, the displacement applied at each step to the lab model was calculated using a numerical step-by-step solution of the corresponding differential equation of motion. The calculated displacement was then applied via a hydraulic actuator, extending the seismic response testing time. The current experimental study, which involved inelastic seismic-response tests of RC column models under simulated strong earthquake excitations and axial loads, was part of a broader research project. This comprehensive project was conducted at the Structural Earthquake Engineering Laboratory at Kyoto University, Japan, and forms part of the third author's PhD dissertation [28]. Seismic tests were carried out using the online computer-controlled Hybrid Loading System for Earthquake Response (HYLSER-1), as shown in Figure 1. Figure 1(a) illustrates the concept of the HYLSER-1 testing system, which consists of three integrated components:

- **the physical part**, including data recording devices that capture the time-history of axial loading at each step (constant in these experiments) and the measured total bending load at each step;
- **the analytical part**, which includes numerical data on the acceleration time-history and intensity of the selected input earthquake, as well as analytically specified mass and damping data for the combined system;
- **the testing laboratory part**, which integrates the laboratory testing equipment, the installed testing model within a compatible mechanical system, and the computer with software that facilitates the step-by-step execution of the HYLSER-1 experiment.

The setup of the RC column model, tested under simulated earthquake excitation and axial loads, is shown in Figure 1(b). The experimental model, labelled "a", was constructed as a simply supported beam with a span divided into three segments of 600 mm each, with the left, middle, and right segments defined by points 1–2, 2–4, and 4–5, respectively. Point 3 represents the middle section of the span, while points 1 and 5 denote the left and right supports from below. The system labelled "b" was used to apply the bending force and record the opposing effective restoring force, which could be positive or negative (±F). The bending force was generated by the electro-hydraulic actuator labelled "1", which was supported by the segment labelled "2". The rigid steel system labelled "3" provided cyclic loading at the symmetrical loading points 2 and 4. The axial force, N1 or N2, was applied using the unbounded (minimised friction) high-strength steel bar labelled "4", installed in a cylindrical space with its central axis aligned with the centroids of the sections along the model length. At its left side, the steel bar was fixed to the concrete face of the model, while on the right side, it was attached to the electro-hydraulic actuator labelled "c", which applied the axial force. When this actuator applied a tensile force to the steel bar, the model experienced a compressive force. The upper points 5 and 6 represent the upper end supports of the model, which are activated when negative (upward) bending forces are applied. The experimental process involved solving a nonlinear second-order differential equation for the combined system, with the restoring force F measured directly from the actuator. The computed incremental displacement for each step was used to determine the total displacement to be applied by the hydraulic actuator. The HYLSER-1 system was successfully used to conduct seismic response tests on the combined system, including the RC column models. Given the complex responses of structural columns as critical elements, dedicated studies on understanding the nonlinear behaviour and seismic safety of both traditional and innovative column types remain a significant and ongoing research topic [29-33].

## 4. Seismic tests of SRC column models including simulated axial loads

### 4.1. Tested SRC column models

All the tested experimental models had a square cross-section of 150 mm × 150 mm, a length of 2100 mm, and a span of 1800 mm, and were constructed using the same type of concrete and longitudinal reinforcement. The longitudinal reinforcement comprised four steel bars (Ø13 mm) with a modulus of elasticity Es = 210.0 GPa and a yield-point stress of fy = 400.0 MPa. The central steel bar (Ø30 mm), used to apply the axial force, was made of high-strength steel with a modulus of elasticity Es = 200.0 GPa and a yield-point stress of fs = 950.0 MPa. Ordinary concrete with a modulus of elasticity of Ec = 27.0 GPa and a compressive strength of fc = 45.0 MPa was used. To study the effect of confinement, transverse reinforcement was provided by spiral steel bars (Ø5 mm) with pitches of e = 6 cm and 9 cm. To investigate the effect of earthquake intensity, three testing intensities were used, defined by the earthquake intensity factor r, with r = 1.0 representing the El Centro "yielding" earthquake, producing a response up to the specimen's yielding point. The intensity was then increased by 30 % and 100 %, represented by r = 1.3 and 2.0, respectively.

### 4.2. Seismic tests with simulated axial load N1 = 88.0 kN

Three seismic tests of steel-reinforced models, subjected to a simulated axial load of N1 = 88.0 kN (0.391 kN/cm$^2$), were conducted using the HYLSER-1 testing system. The design parameters of the tested models and the representative results obtained are presented in Table 1.

For the three pseudo-dynamic tests D1, D6, and D7, the earthquake intensity factors were r = 2.0, 2.0 and 1.3, respectively. In model D1, the spiral reinforcement had a pitch of e = 6.0 cm, whereas models D6 and D7 used a pitch of e = 9.0 cm. The variations in earthquake intensity and confinement resulted in different shapes of the hysteretic

**Table 1. HYLSER-1 tests of normal concrete models: seismic response results for models tested under simulated El Centro earthquake and constant axial load N1 = 88.0 kN**

| Test | | C-Type & EQI (r) | Cylinder $f_{ck}$ [MPa] | Pitch e [cm] | Axial N [kN] | max F +/–[kN] | +/– DM [cm] | +/– FM [kN] | +/– D2 [cm | +/– F2 [kN] |
|---|---|---|---|---|---|---|---|---|---|---|
| 1 | D1 | Normal/ r = 2.0 | 43.4 | 6 | 88.0 | 70.0 | 1.2 | 66.0 | 2.0 | 70.0 |
| | | | | | | -60.0 | -1.1 | -50.0 | -2.0 | -55.0 |
| 2 | D6 | Normal/ r = 2.0 | 49.0 | 9 | 88.0 | 70.0 | 1.1 | 65.0 | 2.0 | 70.0 |
| | | | | | | -60.0 | -1.0 | -50.0 | -2.0 | -55.0 |
| 3 | D7 | Normal/ r = 1.3 | 44.8 | 9 | 88.0 | 70.0 | 1.1 | 68.0 | 2.0 | 70.0 |
| | | | | | | -55.0 | -1.0 | -49.0 | -2.0 | -55.0 |
| Average for e = 6 cm | | | 43.4 | 6 | 88.0 | 65.00 | 1.15 | 58.00 | 2.0 | 62.5 |
| Average for e = 9 cm | | | 46.9 | 9 | | 63.75 | 1.05 | 58.00 | 2.0 | 62.5 |
| Average for e = 6 i 9 cm | | | 45.5 | 6 i 9 | | 64.17 | 1.08 | 58.00 | 2.0 | 62.5 |
| *Analytically predicted | | | | A | 88.0 | 65.00 | 1.00 | 65.00 | 2.0 | 61.0 |

seismic responses. Table 1 provides the following parameters that characterise the hysteretic seismic response:

- max F (+/-): maximum positive and negative restoring forces
- DM (+/-) and FM (+/-): maximum positive and negative deformations and restoring forces at yielding points
- D2 (+/-) and F2 (+/-): for a set deformation of D2 = ±2.0 cm, the recorded positive and negative restoring force at the hysteretic response (HR) contours.

Following the three test rows in Table 1, the next two rows present the average values for models with e = 6.0 cm and 9.0 cm. The subsequent row provides the mean values for all tested models.

The bottom row (marked with *) presents the analytically predicted ultimate force values using the refined micro-model of the tested specimen, based on the pure nonlinear quasi-static analysis described in section 5.5 (1). This analysis considers a transverse reinforcement pitch of e = 6.0 cm. The experimental and analytical results show very good correlation. For instance, the experimentally recorded maximum force (maxF = 64.17 kN) and the analytically predicted maximum force (maxF = 65.0 kN) differ by only 1.3 %. Similarly, for the restoring forces at the identified yielding points, the experimental value (expFM = 58.0 kN) and the analytical value (analFM = 65.0 kN) differ by only 10 %. Present the experimental results comparatively, the hysteretic response (HR) contours of the final seismic responses are used, clearly illustrating the form of the hysteretic response in each specific test. Characteristic points M and L, and M* and L*, denote the yielding point and the point of ultimate deformation response, respectively. Figure 2 shows these representative points on the HR contours for the seismically tested column models D7 and D6, subjected to simulated El Centro earthquakes of different intensities (r = 1.3 and r = 2.0) and a simulated axial load of N1 = 88.0 kN. These two HR contours highlight the effect of earthquake intensity on the hysteretic response, given that other parameters of the structural models remained unchanged.

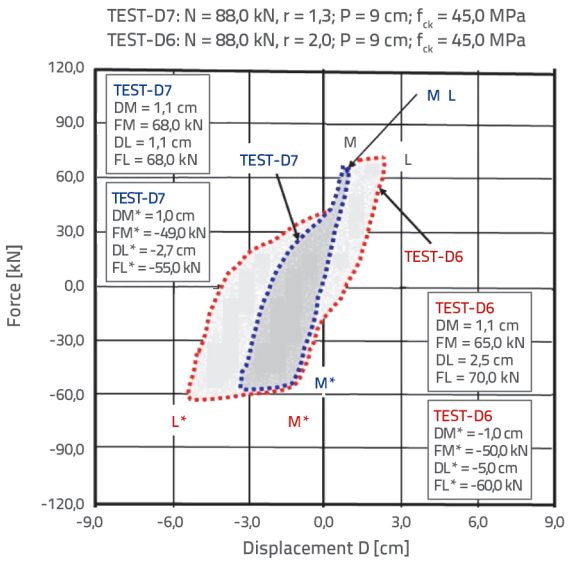


**Figure 2. Representative points and final shapes of hysteretic responses obtained from seismically tested column models D6 and D7, tested under simulated El Centro earthquake with an axial load of N1 = 88.0 kN**

The results in Figure 2 demonstrate that the HYLSER-1 seismic tests are a realistic and highly effective method for verifying the effects of the key parameters influencing the seismic safety of critical elements and structural systems.

### 4.3. Seismic tests with simulated axial load N2 = 265.0 kN

The next five seismic tests of steel-reinforced column models were performed with a larger simulated axial load of N2 = 265.0 kN (1.177 kN/cm$^2$). The parameters of the tested models and their recorded seismic responses are listed in Table 2. Earthquake intensity factor of r = 2.0 was used in tests D2 and D16, r = 1.3

**Table 2. HYLSER-1 tests of normal concrete models: Seismic-response results for models tested under simulated El Centro earthquake with a constant axial load of N2 = 265.0 kN**

| Test | | C-Type & EQI (r) | Cylinder $f_{ck}$ [MPa] | Pitch e [cm] | Axial N [kN] | max F +/– [kN] | +/– DM [cm] | +/– FM [kN] | +/– D2 [cm] | +/– F2 [kN] |
|---|---|---|---|---|---|---|---|---|---|---|
| 1 | D2 | normalan/ r = 2.0 | 49.7 | 6 | 265.0 | 91.0 | 1.5 | 85.0 | 2.0 | 90.0 |
| | | | | | | -81.0 | -1.2 | -78.0 | -2.0 | -80.0 |
| 2 | D3 | normalan/ r = 1.3 | 42.5 | 6 | 265.0 | 90.0 | 1.3 | 74.0 | 2.0 | 90.0 |
| | | | | | | -65.0 | -1.4 | -75.0 | -2.0 | -75.0 |
| 3 | D8 | normalan/ r = 1.3 | 44.8 | 9/ *Urušen* | 265.0 | 87.0 | 1.6 | 87.0 | 2.0 | 80.0 |
| | | | | | | -80.0 | -1.0 | -66.0 | -2.0 | -65.0 |
| 4 | D15 | normalan/ r = 1.0 | 50.1 | 6 | 265.0 | 78.0 | 1.2 | 78.0 | - | Linear |
| | | | | | | -70.0 | -1.0 | -80.0 | - | Linear |
| 5 | D16 | normalan/ r = 2.0 | 61.1 | 6/ *Urušen* | 265.0 | 90.0 | 1.2 | 85.0 | 2.0 | 90.0 |
| | | | | | | -80.0 | -1.2 | -75.0 | -2.0 | -76.0 |
| Average for e = 6 cm | | | 50.85 | 6 | 265.0 | 80.62 | 1.25 | 78.75 | 2.0 | 83.50 |
| Average for e = 9 cm | | | 44.80 | 9 | | 83.50 | 1.30 | 76.50 | 2.0 | 72.50 |
| Average for e = 6 and 9 cm | | | 49.64 | 6 i 9 | | 81.20 | 1.26 | 78.30 | 2.0 | 80.75 |
| * Analytically predicted | | | | A | 265.0 | 82.50 | 1.00 | 80.00 | 2.0 | 60.00 |

was used in tests D3 and D8, and r = 1.0 was used in test D15, respectively. The transverse spiral reinforcements used in Models D2, D3, D15, and D16 had a pitch of e = 6.0 cm, whereas e = 9.0 cm was used in Model D8. Table 2 lists the experimentally obtained parameters that controlled the seismic responses of the five tested models. After the five separate test rows of Table 2, the next three rows give the average values for the models with e = 6.0 cm and 9.0 cm, as well as the average values for all five tested models. Similarly, the bottom row (marked with *) presents the analytically predicted ultimate force values using the same refined micromodel of the specimen and the nonlinear quasi-static analysis described in Section 5.5. (2), considering the pitch e = 6.0 cm for the transverse reinforcement. Again, there is a strong correlation between the analytical and experimental results. Specifically, the difference between the maximum restoring forces defined experimentally and analytically was 1.6 %, and for the restoring forces at the yield point, the recorded difference of 2.2 % was also very small. Representative HR contours were constructed for the tests performed under the simulated effects of an axial load of N2 = 265.0 kN. Analogously, the HR contours are presented as points M, L, M*, and L*, which control the shapes of the recorded seismic responses. Figure 3 shows the stable hysteretic responses obtained for the seismically tested column models D15 and D2 under the simulated El Centro earthquake with defined intensities represented by r = 1.0 and 2.0, respectively.

For model D2, the obtained HR contours were rather wide and expressed strong nonlinear behaviour owing to the simulated high earthquake intensity, represented by r = 2.0. However, the seismic response of model D15 was mainly linear and only reached the yielding point on the sides of the positive and negative deformations. This experiment confirms that with r = 1.0, the seismic response exhibits linear behaviour. Models D2 and D15 exhibited stable hysteretic responses owing to the smaller pitch of the spiral reinforcement (e = 6.0 cm). Figure 4 shows the representative points on the HR contours for seismically tested column models D3 and D8 with the same earthquake input intensity (r = 1.3). Model D3 exhibited a stable hysteretic response, whereas model D8 collapsed, as manifested by the measured zero restoring force. This large difference in the seismic responses of models D3 and D8 is directly due to the difference in confinement, with pitches of e = 6.0 cm and 9.0 cm used for models D3 and D8, respectively.

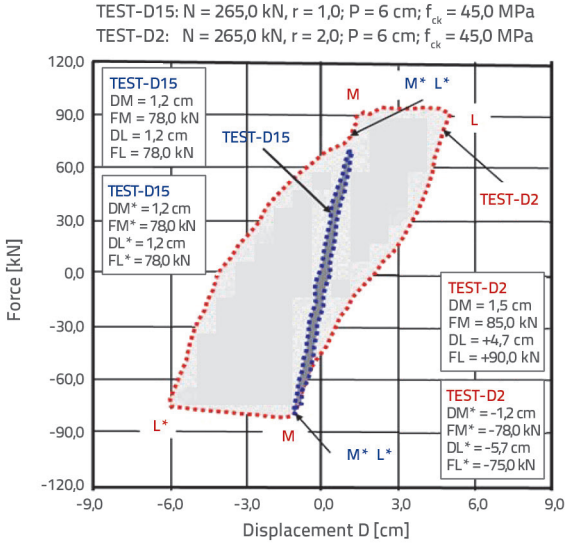


**Figure 3. Representative points and final shapes of hysteretic responses obtained from seismically tested column models D15 and D2, subjected to the El Centro earthquake and an axial load of N2 = 265.0 kN**

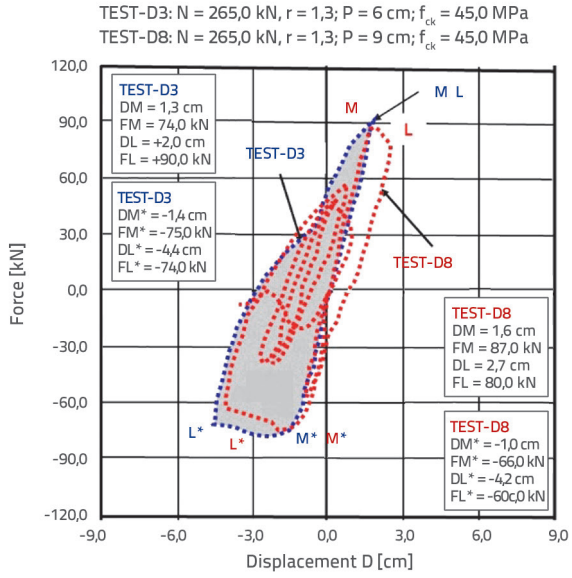


**Figure 4. Representative points and final shapes of hysteretic responses obtained from seismically tested column models D3 and D8 under simulated El Centro earthquake and axial load N2 = 265.0 kN**

## 5. Refined nonlinear modelling of steel- and GFRP-reinforced columns

A key component of the present research involved an independent refined analytical simulation of a typical quasi-static test, or performing an "analytical experiment" (analysis with simulated time-dependent loading). This analytical study defined the comparative hysteretic responses of column models with identical geometry, support, and loading conditions, similar to the tested specimens. Two comparative analyses were carried out, considering column models reinforced with either conventional steel or novel GFRP reinforcement. This analysis was successfully completed, drawing on the authors' previous experience with refined modelling. Specifically, refined and experimentally validated three-dimensional nonlinear analytical models used in prior research [14, 15] were applied. This study serves as complementary research, providing additional insights into the specimens' hysteretic responses that were not captured in the HYLSER-1 seismic tests. The hysteretic response in the "analytical test" was obtained using predefined cyclic loading, while in the HYLSER-1 test, the cyclic loading is random, depending on earthquake intensity and frequency content.

### 5.1. Material properties

Table 3 details the steel and GFRP reinforcements of the analytically studied columns, as well as the simulated bending and axial loading programs.
Table 4 lists the properties of the ordinary steel reinforcement and Table 5 lists those of the novel GFRP bars, which define the respective stress–strain relations as adopted from tests presented previously [14, 15].

### 5.2. Nonlinear finite-element analysis model

The conducted nonlinear finite-element analysis (FEA) was focused on advancing the modelling of the two types of tested specimens, that is column models reinforced with (i) ordinary steel and (ii) composite GFRP reinforcing bars, simulating the same loading protocol up to the highly nonlinear behaviour state. Because the adopted complex earthquake-like loading protocol represents simultaneous constant axial and reverse cyclic shear loadings, a nonlinear analytical study is a complex task. To capture the complex

**Table 3. Modelling and loading of analysed columns with details of the steel and GFRP reinforcements**

| Model | Reinforcement type | Longitudinal bars Ø [mm] | Transversal spiral bars Ø [mm] | Loading of models (Analytical test) | |
|---|---|---|---|---|---|
| | | | | Axial-constant (compressive) | Bending (displacement) |
| M1 | steel | 4Ø13 | Ø5/6 cm | 88.0 kN | cyclic |
| M2 | steel | 4Ø13 | Ø5/6 cm | 265.0 kN | cyclic |
| M1A | GFRP | 4Ø10 | Ø5/6 cm | 88.0 kN | cyclic |
| M2A | GFRP | 4Ø10 | Ø5/6 cm | 265.0 kN | cyclic |

**Table 4. Mechanical properties of the steel reinforcing bars**

| Diameter [mm] | Material | Tensile elastic modulus Es [GPa] | Yield strength fy [MPa] | Ultimate strength [MPa] | Yield strain [%] | Elongation [%] |
|---|---|---|---|---|---|---|
| 13 | čelik | 210 | 400 | 560 | 0.2 | 5 |

**Table 5. Mechanical properties of the GFRP reinforcing bars**

| Diameter [mm] | Material | Tensile elastic modulus [GPa] | Tensile strength [MPa] | Ultimate strain in tension [%] |
|---|---|---|---|---|
| 10 | GFRP | 50 | 1100 | 2.5 |

response phenomena, a fibre section technique was implemented using *SeismoStruct software* [34]. The column specimen was modelled using four 3D nonlinear fibre-based finite elements spaced between *five nodal points*. To capture the curvature distribution along each finite element realistically, *five added integration sections* per element were considered. SeismoStruct only provides access to the stress–strain fibre response at the element end sections. The model cross-sections were discretised into a refined fibre mesh considering the fibres for the *confined* concrete, *unconfined* concrete, and actual *reinforcing fibres*.

### 5.3. Material stress–strain modelling

To model the nonlinear behaviour of concrete, the Chang and Mander (1994) model was selected. This model used a mean compressive strength of 48.0 MPa, a mean tensile strength of 4.8 MPa, a modulus of elasticity of 32,562.5 MPa, and a strain at peak stress of 0.002. Non-dimensional critical compressive and tensile strain coefficients determined the shape of the hysteretic curve. For the nonlinear behaviour of steel reinforcement, the Menegoto–Pinto steel model [34] was employed, with a modulus of elasticity of $2 \times 10^5$ MPa and a yield strength of 575.0 MPa. The behaviour of the GFRP reinforcement bars was modelled using a linear model with a modulus of elasticity of $5 \times 10^4$ MPa, a tensile strength of $1.1 \times 10^3$ MPa, a compressive strength of $7 \times 10^2$ MPa and a specific weight of 50 kN/m$^3$.

### 5.4. Numerical nonlinear stress–strain analysis strategy

The refined numerical nonlinear stress–strain analysis strategy was established by carefully selecting the following key parameters:

- a total of 800 solution steps, with a time step of dt = 0.005 s, resulting in a total pseudo-solution time of T = 4.4 s
- an iterative strategy with a maximum of 40 iterations per solution increment (IT = 40), up to 35 updates of the tangent stiffness matrix per increment (NSA = 35), a divergence iteration limit of (DI = 35), a maximum tolerance criterion set to $1 \times 10^{20}$ (maxT = 1e20), a maximum step reduction of 0.001 (maxSR = 0.001) and a minimum of 1 solution iteration (minSI = 1)
- updated convergence criteria, using a mixed displacement/rotation-based approach with a displacement tolerance of 0.0001 m and a rotation tolerance of 0.0001 rad. Throughout the analytical study, a maximum of three iterations per step was conducted during the computational process.

### 5.5. Modelling of columns with ordinary steel reinforcement

**1) Ordinary steel reinforced column with simulated axial load N1 = 88.0 kN.** The analytically predicted hysteretic force–displacement response of column model M1 reinforced with ordinary steel bars under simulated cyclic bending and a constant axial load of N1 = 88.0 kN is shown in Figure 5. The computed hysteretic relation has a fully symmetrical shape, which is directly confirmed by the constructed positive branch of the envelope line defined by points Y, U, and L and the symmetric negative branch defined by the respective symmetric points (blue line). The initial stiffness is represented by the first-line segment. Owing to the simulated effect of the lower axial load N1, the deciding part of the envelope defined by points U and L is not sharp and generally exhibits very good ductile behaviour.

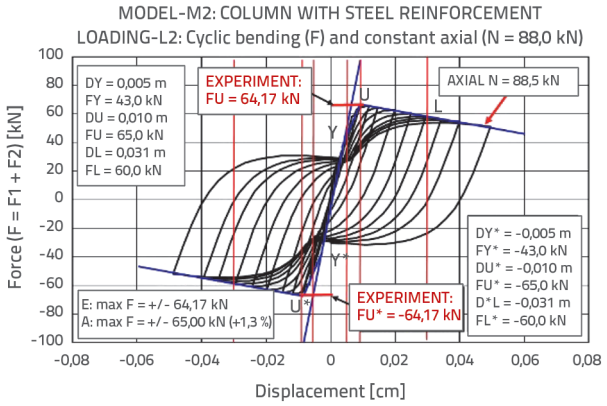


**Figure 5. Model M1 with steel reinforcement: Analytically predicted hysteretic force–displacement response under simulated cyclic bending and constant axial load N1 = 88.0 kN**

**2) Ordinary steel reinforced column with simulated axial load N2 = 265.0 kN.** The analytically predicted hysteretic force–displacement response of column model M2 reinforced with ordinary steel bars under simulated cyclic bending and a constant axial load of N2 = 265.0 kN is shown in Figure 6.

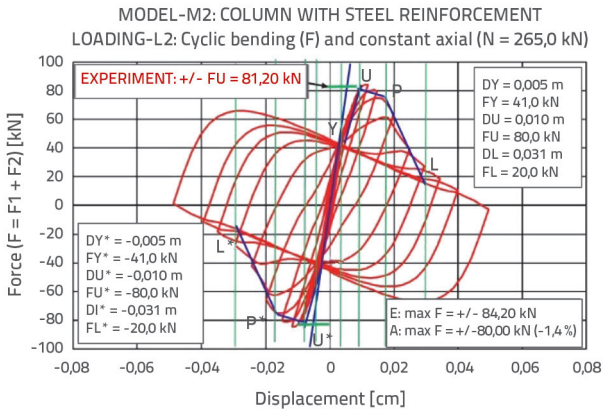


**Figure 6. Model M2 with steel reinforcement: Predicted hysteretic response under simulated cyclic bending and constant axial load N2 = 265.0 kN**

Owing to the simulated effect of the higher axial load N2, the deciding part of the envelope line defined by points U and L became very sharp, indicating poor ductility.

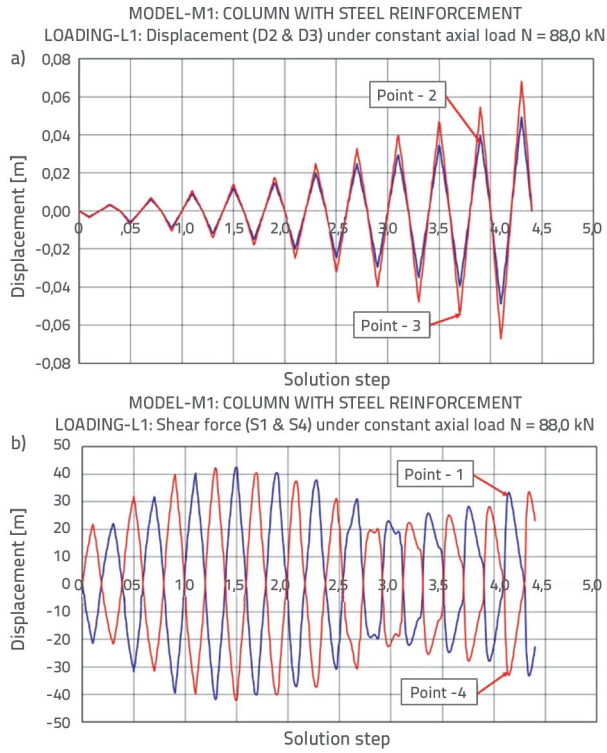


**Figure 7. Model M1 with steel reinforcement: Displacement and shear force histories under simulated cyclic bending and constant axial load N1 = 88.0 kN**

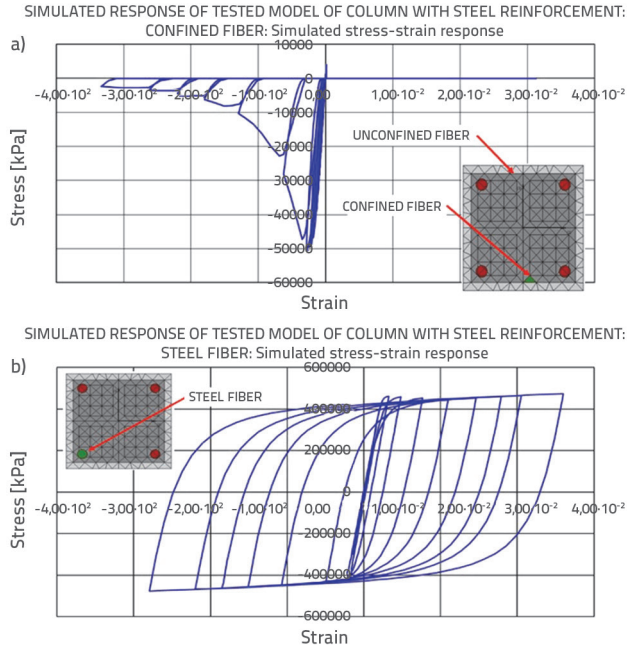


**Figure 8. Model M1 with steel reinforcement: Stress–strain relationships of confined concrete and steel fibres under cyclic bending and constant axial load N1 = 88.0 kN, (stress: kPa)**

Figure 7 shows the predicted characteristic displacement and shear force histories under the simulated cyclic bending and constant axial load N1 = 88.0 kN, and Figure 8 shows examples of the monitored and plotted stress–strain relations of the selected confined concrete fibre and ordinary streel reinforcing fibre.

## 5.6. Modelling of columns with composite GFRP reinforcement

**1) Composite GFRP reinforced column with simulated axial load N1 = 88.0 kN.** The hysteretic response obtained by analysing the equivalent column model M1A reinforced with composite GFRP reinforcement under simulated cyclic bending and constant axial load N1 = 88.0 kN is presented in Figure 9 (green).

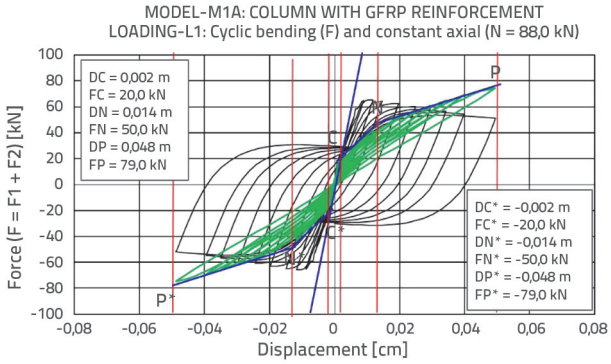


**Figure 9. Model M1A with glass fibre-reinforced polymer (GFRP) bars: Hysteretic response under simulated cyclic bending and constant axial load N1 = 88.0 kN. The model with composite reinforced concrete (CRC) is shown in green, and the model with steel reinforced concrete (SRC) is shown in black**

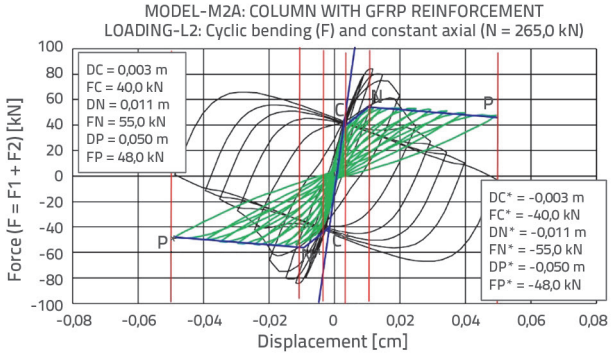


**Figure 10. Model M2A with GFRP reinforcement: Hysteretic response under simulated cyclic bending and constant axial load N2 = 265.00 kN. The model with composite reinforced concrete (CRC) is shown in green, and the model with steel reinforced concrete (SRC) is shown in black**

Compared with the steel reinforcement (black), the computed hysteretic relationship in this case is quite different but still maintains a fully symmetrical shape. This is illustrated by the positive branch of the envelope line, defined by points C, N, and P, and the corresponding negative branch, defined by points C*, N* and P*.

Owing to the simulated effect of the lower axial load N1, the final segment of the line defined by points N and P exhibits low stiffness, with a positive slope even for very large deformations. However, it is crucial to note that the hysteretic response is characterised by a significant pinching effect, resulting from the combined effects of the linear response of the GFRP bars and the nonlinear stress–strain response of the concrete fibres.

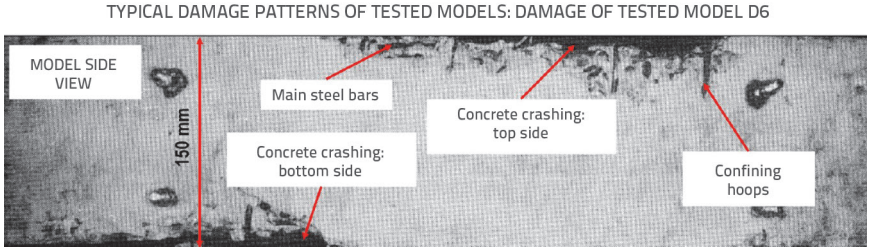


**Figure 11. Side view of the recorded damage to the middle section of the tested RC model D6 (old photograph)**

**2) Composite GFRP reinforced column with simulated axial load N2 = 265.0 kN.** Similarly, Figure 10 (green) shows the analytically predicted hysteretic response for the analysed column model M2A, which is reinforced with the same composite GFRP reinforcement and subjected to simulated cyclic bending and a constant axial load N2 = 265.0 kN.

Compared to the hysteresis observed for the lower axial load N1, the shape of the hysteretic response for the larger axial force N2 differs significantly. This is evident in the positive branch of the envelope line, defined by points C, N, and P, and the symmetric negative segment, defined by points C*, N* and P*. Due to the higher axial load N2, the segment defined by points N and P exhibits small but stable negative stiffness, indicating very high ductility for large deformations. Nonetheless, the predicted hysteretic response also demonstrates a pronounced pinching effect.

## 6. Main findings

**1) Damage.** An important advantage of the HYLSER-1 seismic tests was that the test execution time was extended to approximately 45 min, which was used to monitor the crack and damage propagation during the characteristic model response phases. As shown in Figure 11, typical damage was observed in the critical (middle) part of the tested model D6 (side view). The propagation of the initial and wider cracks and crushing or spalling of the concrete were always observed at the bottom and top faces of the deformed specimens. Similar damage locations were identified in an analytical study. This was confirmed by the plotted stress-strain relations for the concrete and steel fibres at the critical section.

**2) Model.** The original results obtained from the HYLSER-1 seismic tests validated the numerical modelling strategy. Figure 12 shows the maximum shear forces obtained from three HYLSER-1 seismic tests of the RC models and the analytically predicted shear force under simulated cyclic bending and constant axial load N1 = 88.0 kN; the recorded differences are very small, being 4 % at most, in this case. Similarly, Figure 13 shows the maximum shear forces obtained from five HYLSER-1 seismic tests of RC models and the analytically predicted shear force under simulated cyclic bending and identical axial load N2 = 265.0 kN; In this case, the recorded differences are also very small, 11.4 % at most.

**3) Effects of axial load.** The shape of the hysteretic response of the columns reinforced with steel or GFRP bars was strongly affected by the axial load level. For columns reinforced with steel bars, the maximum restoring forces obtained under simulated axial load levels N1 and N2 were 65.0 kN and 80.0 kN, respectively, and the resulting difference of 23.1 % is significant. The shapes of the HC contours also differ (Figures 5 and 6). For columns reinforced with GFRP bars, the restoring forces recorded under simulated axial loads N1 and N2 were 40.0 kN and 55.0 kN, respectively, and the obtained difference of 37.5 % is also significant. The HC contour shapes were also significantly affected (Figures 9 and 10).

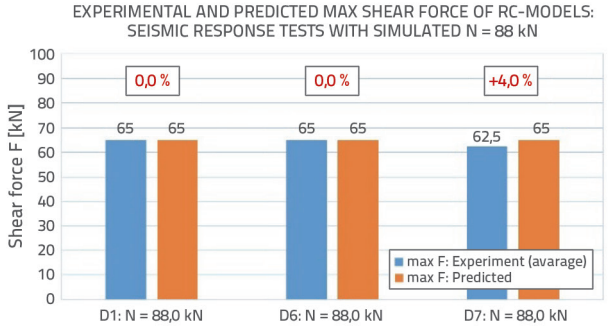


**Figure 12. Maximum shear forces from three HYLSER-1 seismic tests of RC models compared with analytical predictions, with simulated axial load N1 = 88.0 kN**

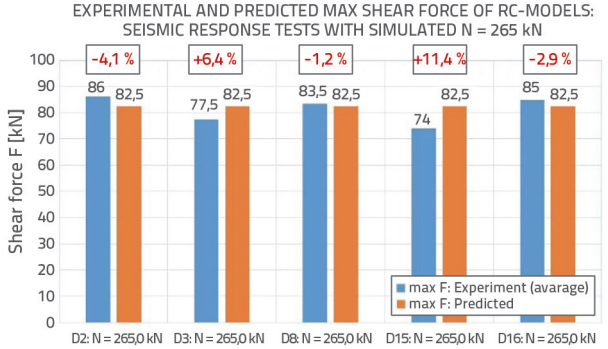


**Figure 13. Maximum shear forces from five HYLSER-1 seismic tests of RC models compared with analytical predictions, with simulated axial load N2 = 265.0 kN**

**4) Stiffness and deformability.** The difference in the stiffness characteristics of the columns reinforced with steel and GFRP bars was significant. For columns reinforced with steel bars, the recorded stiffness was much larger than that of columns reinforced with GFRP bars (Figures 5, 6, 9, and 10), and the results indicated that columns reinforced with GFRP bars were exposed to larger deformations.

## 7. Conclusions

Based on the results from the extensive experimental seismic tests and advanced analytical study reported herein, the following conclusions are drawn, relevant to the successful seismic design of columns reinforced with either ordinary steel bars or novel GFRP bars:

- The relatively small variations in concrete strength (approximately 8 %–12 %) observed in this study had a minimal impact on the hysteretic response of the tested RC column models.
- For columns tested under a lower axial force (N1), the effect of different levels of confinement on their hysteretic response was negligible. However, under a larger simulated axial force (N2), significant damage or collapse of the RC columns was recorded, particularly under earthquakes of higher intensity.
- For columns reinforced with either steel or GFRP, varying levels of axial force had a substantial impact. Under lower simulated axial forces, the hysteretic behaviour remained stable and generally exhibited pronounced ductility. However, under higher simulated axial forces, the hysteretic behaviour showed reduced ductility, rapidly decreasing restoring force, significant damage, and eventual failure, especially under higher earthquake intensities.
- Both experimental and analytical investigations confirmed that critical behaviour or total collapse of steel- or GFRP-reinforced columns occurs when the level of confinement is inadequate and the columns are subjected to high axial forces generated by intense earthquakes.
- The study confirmed that while steel-reinforced columns demonstrate a significantly higher capacity for energy absorption, GFRP-reinforced columns exhibit much lower capacity due to the pronounced pinching effect observed in their hysteretic seismic response.
- For future design of steel-reinforced columns in seismic areas, it is crucial to estimate and account for potential variations in axial force.
- For future design of columns reinforced with novel GFRP bars in seismic areas, it is essential to reliably evaluate the potential variable levels of axial force and the effects of increased deformability under seismic loads, and to incorporate these considerations into the design.

## Acknowledgements

Seismic HYLSER-1 tests were performed at the Structural Earthquake Engineering Laboratory of Kyoto University, Japan, whereas extended GFRP-related tests and analytical research were performed at the RESIN Laboratory, Skopje, established as a regional research centre by Prof. D. Ristic, PPD, in the framework of the innovative NATO Science for Peace and Security Project: *Seismic upgrading of Bridges in South-East Europe by Innovative Technologies (SFP: 983828).* The authors express their sincere thanks to both laboratories for their extended support and testing conditions.

## REFERENCES

[1] Raza, S., Scott, J., Menegon, J., et al.: Axial Load Variation of Columns in Symmetrical RC Buildings Subject to Bidirectional Lateral Actions in Regions of Low to Moderate Seismicity, Journal of Earthquake Engineering, 2020, https://doi.org/10.1080/13632469.2020.1772151

[2] Di Ludovico, M., Verderame, G.M., Prota, A., et al.: Experimental behaviour of nonconforming RC columns with plain bars under constant axial load and biaxial bending, Journal of Structural Engineering, 139 (2013) 6, pp. 897–914, https://doi.org/10.1061/(ASCE)ST.1943-541X.0000703.

[3] Qiu, F.W., Li, W.F., Pan, P., et al.: Experimental tests on reinforced concrete columns under biaxial quasi-static loading, Engineering Structures, 24 (2002) 4, pp. 419–28. https://doi.org/10.1016/S0141-0296(01)00108-0.

[4] Raza, S., Menegon, S.J., Tsang, H.H., et al.: Force-displacement behaviour of limited ductile high-strength RC columns under bidirectional earthquake action,. Engineering Structures, 208 (2020), pp. 110278. https://doi.org/10.1016/j.engstruct.2020.110278.

[5] Rodrigues, H., Arêde, A., Varum, H., et al.: Experimental evaluation of rectangular reinforced concrete column behaviour under biaxial cyclic loading, Earthquake Engineering and Structural Dynamics, 42 (2013) 2, pp. 239–59, https://doi.org/10.1002/eqe.2205.

[6] Rodrigues, H., Varum, H., Arêde, A., et al.: A comparative analysis of energy dissipation and equivalent viscous damping of RC columns subjected to uniaxial and biaxial loading, Engineering Structures, 35 (2012), pp. 149–64, https://doi.org/10.1016/j.engstruct.2011.11.014.

[7] Raza, S., Tsang, H.H., Wilson, J.L.: Unified models for post-peak failure drifts of normal- and high-strength RC columns. Magazine of Concrete Research, 70 (2018) 21, pp. 1081–1101.

[8] Raza, S., Menegon, S.J., Tsang, H.H., et al.: Collapse performance of limited ductile high-strength RC columns under uni-directional cyclic actions, Journal of Structural Engineering, 2020a, https://doi.org/10.1061/(ASCE)ST.1943-541X.0002772.

[9] Wilson, J.L., Wibowo, A., Lam, N.T.K., et al.: Drift behaviour of lightly reinforced concrete columns and structural walls for design applications, Australian Journal of Structural Engineering, 16 (2015) 1, pp. 62–73, https://doi.org/10.7158/S14-002.2015.16.1.

[10] Menegon, S.J., Wilson, J., Lam, L., et al.: RC walls in Australia: Seismic design and detailing to AS 1170.4 and AS 3600. Australian Journal of Structural Engineering, 19 (2018) 1, pp. 67–84, https://doi.org/10.1080/13287982.2017.1410309.

[11] He, R., Yang, Y., Sneed, L.H.: Seismic repair of reinforced concrete bridge columns: Review of research findings. Journal of Bridge Engineering, 20 (2015) 12, pp. 04015015, https://doi.org/10.1061/(ASCE)BE.1943-5592.0000760.

[12] Raza, S., Khan, M.K.I., Menegon, S.J., et al.: Strengthening and repair of reinforced concrete columns by jacketing: State-of-the-art review, Sustainability, 11 (2019) 11, pp. 3208. https://doi.org/10.3390/su11113208.

[13] De Luca, A., Matta, F., Nanni, A.: Behavior of full-scale concrete columns internally reinforced with glass FRP bars under pure axial load, Composites & Polycon 2009, American Composites Manufacturers Association, January 15-17, 2009.

[14] Guri, Z., Kokalanov, G., Ristic, D., Ristic, J.: Modeling of circular columns with ordinary and composite reinforcement, Proceedings of International conference: Earthquake engineering and engineering seismology, SGIS, 2018, Kraljevo, Serbia.

[15] Guri, Z., Misini, M.: Experimental testing and numerical analysis of circular columns reinforced with steel and glass-fibre-reinforced polymer. Magazine of Concrete Research, 73 (2019) 4, pp.1-27, https://doi.org/10.1680/jmacr.19.00003.

[16] ACI (American Concrete Institute): ACI 440.1R-06: Guide for the design and construction of concrete reinforced with FRP bars. Committee 440, American Concrete Institute, Farmington Hills, MI, USA, 2006.

[17] CSA (Canadian Standards Association): CAN/CSA-S806-02: Design and Construction of Building Components with Fibre Reinforced Polymers. Canadian Standards Association, Toronto, Ontario, Canada, 2002.

[18] Deitz, D.H., Harik, I.E., Gesund, H.: Physical properties of glass fiber reinforced polymer rebars in compression. Journal of Composites for Construction, 7 (2003) 4, pp. 292–301.

[19] Tobbi, H., Farghaly, A.S., Benmokrane, B.: Concrete columns reinforced longitudinally and transversally with glass fiber-reinforced polymer bars, ACI Structural Journal, 109 (2012) 4, pp. 551–558.

[20] Hadi, M., Karim, H., Sheikh, M.: Experimental investigations on circular concrete columns reinforced with GFRP bars and helices under different loading conditions, Journal of Composites for Construction, 20 (2016) 4, pp. 4016009-1-04016009-12.

[21] Elchalakani, M., Ma, G., Aslani, F., Duan W.: Design of GFRP-reinforced rectangular concrete columns under eccentric axial loading. Magazine of Concrete Research, 69 (2017) 17, pp. 1-13.

[22] Weber, A.: Advanced reinforcement technology with GFRP rebar. In Proceedings of the 2nd International fib Congress, Naples, Italy, 2006.

[23] Nanni, A.: Flexural behavior and design of RC members using FRP reinforcement, Journal of Structural Engineering, 119 (1993) 11, pp. 3344–3359.

[24] Takanashi, K., et al.: A Simulation of Earthquake Response of Steel Buildings In Proceedings, 6th World Conference on Earthquake Engineering, New Delhi, India, 1997.

[25] Takanashi, K., et al.: Pseudo-Dynamic Tests on 2-Story Steel Frame by Computer-Load Test Apparatus Hybrid System In Proceedings, 7th World Conference on Earthquake Engineering. Istanbul, Turkey, 1981.

[26] Okada, T., Seki, M., Park, Y.J.: A Simulation of Earthquake Response of Reinforced Concrete Building Frames to Bi-Directional Ground Motion by IIS Computer-Actuator On-Line System. In Proceedings of the 7th World Conference on Earthquake Engineering, Istanbul, Turkey, 1980.

[27] Yamada, Y., Iemura, H.: Hybrid Analysis on Earthquake Response of Deteriorating Hysteretic Structures, In Proceedings of the Sino-American Symposium on Bridge and Structural Engineering, Peking, China, 1982.

[28] Ristic, D.: Nonlinear behavior and stress-strain based modelling of reinforced concrete structures under earthquake induced bending and varying axial loads, Doctoral Dissertation, School of Civil Engineering, Kyoto University, Japan, 1988.

[29] Tamahloult, M., Tiliouine, B.: 3D nonlinear seismic analysis and design of base-isolated buildings under near field ground motions, GRAĐEVINAR, 75 (2023) 5, pp. 483-493, https://doi.org/10.14256/JCE.3548.2022

[30] Başgöze, A., Güncü, A.: Determining the regional disaster risk analysis of buildings in Erzincan, GRAĐEVINAR, 75 (2023) 3, pp. 257-272, https://doi.org/10.14256/JCE.3436.2021

[31] Husain, M., Hassan, H., Mohamed, H.A., Elgharbawy, E.S.: Seismic response of post-tension shear walls – Outrigger structure, GRAĐEVINAR, 74 (2022) 6, pp. 491-502, https://doi.org/10.14256/JCE.3418.2021

[32] Mertol, H. C., Tunc, G., Akis, T.: Evaluation of masonry buildings and mosques after Sivrice earthquake, GRAĐEVINAR, 73 (2021) 9, pp. 881-892, https://doi.org/10.14256/JCE.3101.2021

[33] Kišiček, T., Stepinac, M., Renić, T., Hafner, I., Lulić, L.: Strengthening of masonry walls with FRP or TRM, GRAĐEVINAR, 72 (2020) 10, pp. 937-953, https://doi.org/10.14256/JCE.2983.2020

[34] SeismoStruct: SeismoStruct – A computer program for static and dynamic nonlinear analysis of framed structures Seismosoft, Pavia, Italy, 2021, http://www.seismosoft.com/en/SeismoStruct.aspx